AD-A181 651 RELATIVISTIC SELF FOCUSING OF SHORT PULSE RADIATION BEAMS IN PLASMAS(U) BERKELEY SCHOLARS INC SPRINGFIELD VA P SPRANGLE ET AL. 15 MAY 87 NLR-MR-5962 1/1

UNCLASSIFIED F/G 20/3 NL

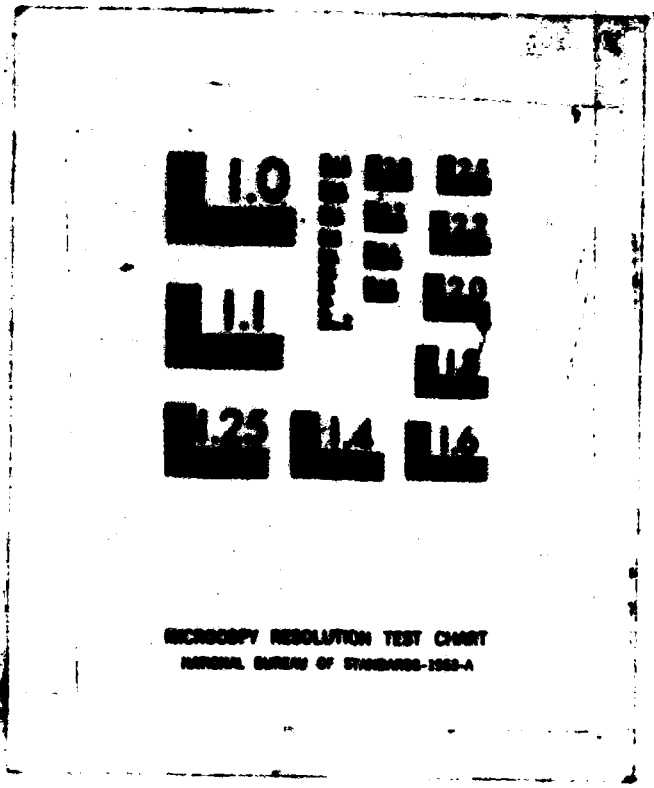
1.0
1.1
1.25
1.4
1.6
MICROCOPY RESOLUTION TEST CHART
NATIONAL BUREAU OF STANDARDS-1963-A

Naval Research Laboratory
Washington, DC 20375-5000

NRL Memorandum Report 5962

Relativistic Self Focusing of Short Pulse Radiation Beams in Plasmas

P. SPRANGLE, CHA-MEI TANG, AND E. ESAREY*

Plasma Theory Branch
Plasma Physics Division

Berkeley Scholars, Inc.
P.O. Box 852
Springfield, VA 22150

May 15, 1987

AD-A181651

SECURITY CLASSIFICATION OF THIS PAGE

REPORT DOCUMENTATION PAGE

1a. REPORT SECURITY CLASSIFICATION UNCLASSIFIED	1b. RESTRICTIVE MARKINGS
2a. SECURITY CLASSIFICATION AUTHORITY	3. DISTRIBUTION/AVAILABILITY OF REPORT Approved for public release; distribution unlimited.
2b. DECLASSIFICATION/DOWNGRADING SCHEDULE	
4. PERFORMING ORGANIZATION REPORT NUMBER(S) NRL Memorandum Report 5962	5. MONITORING ORGANIZATION REPORT NUMBER(S)
6a. NAME OF PERFORMING ORGANIZATION Naval Research Laboratory	6b. OFFICE SYMBOL (If applicable) Code 4790
6c. ADDRESS (City, State, and ZIP Code) Washington, DC 20375-5000	7a. NAME OF MONITORING ORGANIZATION
8a. NAME OF FUNDING/SPONSORING ORGANIZATION U.S. Department of Energy	8b. OFFICE SYMBOL (If applicable)
8c. ADDRESS (City, State, and ZIP Code) Washington, DC 20545	7b. ADDRESS (City, State, and ZIP Code)
	9. PROCUREMENT INSTRUMENT IDENTIFICATION NUMBER
	10. SOURCE OF FUNDING NUMBERS PROGRAM ELEMENT NO.: DOE; PROJECT NO.: A105-83 ER40117; TASK NO.: ORD (326); WORK UNIT ACCESSION NO.: DN380-537

11. TITLE (Include Security Classification)
Relativistic Self Focusing of Short Pulse Radiation Beams in Plasmas

12. PERSONAL AUTHOR(S)
Sprangle, P., Tang, Chia-Mei, and Esarey,* E.

13a. TYPE OF REPORT	13b. TIME COVERED	14. DATE OF REPORT (Year, Month, Day)	15. PAGE COUNT
Interim	FROM ____ TO ____	1987 May 15	39

16. SUPPLEMENTARY NOTATION
*Berkeley Scholars, Inc., P.O. Box 852, Springfield, VA 22150

17. COSATI CODES		
FIELD	GROUP	SUB-GROUP

18. SUBJECT TERMS (Continue on reverse if necessary and identify by block number)
(Relativistic) self-focusing, Envelope equation, Laser-plasma interactions, Relativistic plasma, Radiation propagation

19. ABSTRACT (Continue on reverse if necessary and identify by block number)

An envelope equation is derived which describes the radial evolution of a radiation beam propagating through a plasma. The radiation envelope equation contains a defocusing term due to diffraction spreading and a focusing term due to relativistic oscillations of the plasma electrons. The case of a constant density background plasma is analyzed in detail and an expression for a critical laser power is derived. For powers exceeding the critical power the radiation envelope oscillators and does not diffract. Under certain conditions, the radiation beam propagates through the plasma with a constant radius envelope.

20. DISTRIBUTION/AVAILABILITY OF ABSTRACT	21. ABSTRACT SECURITY CLASSIFICATION
☒ UNCLASSIFIED/UNLIMITED ☐ SAME AS RPT. ☐ DTIC USERS	UNCLASSIFIED
22a. NAME OF RESPONSIBLE INDIVIDUAL P. Sprangle	22b. TELEPHONE (Include Area Code) (202) 767-3493
	22c. OFFICE SYMBOL Code 4790

DD FORM 1473, 84 MAR 83 APR edition may be used until exhausted. All other editions are obsolete

SECURITY CLASSIFICATION OF THIS PAGE

CONTENTS

RELATIVISTIC SELF FOCUSING OF SHORT PULSE RADIATION BEAMS IN PLASMAS

The interaction of intense radiation beams with plasmas plays an important role in such areas as laser driven fusion, ionospheric processes and pulsar radiation. Recently the possibility of employing intense laser beams to accelerate electrons to ultra-high energies has also stimulated interest in radiation self-focusing in plasmas.[1-14] One such laser driven acceleration scheme is the laser beat wave accelerator. This is a collective acceleration scheme which utilizes a large amplitude plasma wave with phase velocity slightly less than the velocity of light to accelerate charged particles. The large amplitude plasma wave is excited by the nonlinear coupling of two intense laser beams propagating through the plasma. In this process the two laser beams with frequencies ω_1, ω_2 and corresponding wave numbers k_1, k_2 couple through the plasma to produce a ponderomotive wave with frequency $\omega_1 - \omega_2$ and wave number $k_1 - k_2$. If $\omega_1 - \omega_2 = \omega_{pe}$, the plasma wave will initially grow linearly in time. If the laser frequencies are much greater than the ambient plasma frequency, ω_{pe}, then the phase velocity of the ponderomotive wave is nearly equal to the group velocity of the laser wave. Electrons which are either injected into the plasma or part of the thermal tail of the plasma distribution can be accelerated by the large gradients associated with the plasma wave.

In this paper the self-focusing properties of a plasma on an intense electromagnetic beam are studied.[15-22] The propagation of an intense radiation beam in a plasma can result in self-focusing by creating a density depression in the plasma as well as by increasing the electron mass by relativistic effects. The density depression is due to transverse ponderomotive forces which tend to expel plasma from high field regions. The radial ponderomotive force on the electrons is larger than on the ions by the

Manuscript approved January 20, 1987.

[illegible]. The electrons forced out of the radiation beam region set up an electrostatic restoring force which, on a slower time scale, causes the ions to be expelled. The charge separation which sets up the electrostatic restoring force extends over a Debye length which is assumed small compared to the radiation beam radius. This density depression creates a local increase in the effective index of refraction and acts as an optical guide for the radiation beam. In addition to this self-focusing mechanism a further reduction in the plasma frequency occurs in regions of high field intensity due to the relativistic mass increase of the electrons in the presence of the radiation beam. The self-focusing due to the density depression occurs on a longer time scale than does the relativistic mass increase self-focusing effect. When the ponderomotive pressure is much less than the plasma kinetic pressure the time scale for the density depression to occur is $\tau_s = R/C_s$, where R is the radiation beam radius and C_s is the ion acoustic speed. Since R is assumed much greater than the Debye length, the characteristic time is greater than the ion time scale ($\tau_s >> \omega_{pi}^{-1}$). On the other hand, the time scale for the relativistic mass increase is $\tau_R = \omega^{-1}$ where ω is the radiation frequency and is assumed much greater than the electron plasma frequency.

Previous research on self-focusing was primarily concerned with the ponderomotive self-focusing effect.[15-17] Max[15] presented steady-state solutions for the radiation beam structure due to ponderomotive self-focusing in a nonrelativistic plasma. In this treatment it was assumed that the plasma had attained equilibrium with the radiation field and, hence, the plasma density was represented by a Boltzman-type response, $n = \exp(e\phi_p/T_e)$, where ϕ_p is the ponderomotive potential and T_e is the electron temperature. Felber[16] performed a similar treatment of ponderomotive self-focusing with the inclusion of relativistic effects and, again, the assumption of an equilibrium

[illegible]-type density distribution was used. Such treatments, using an [illegible] density response, are invalid for short radiation pulses, $\tau < [illegible]$. On such short time scales, the plasma ions can not respond to the [illegible] force.

The problem of relativistic self-focusing alone, valid for short times before the ion density responds to ponderomotive force, has been considered by Max et al.,[18] Sprangle and Tang[19] and Schmidt and Horton.[20] Numerical simulations have also been attempted for arbitrary times including the combined effects of relativistic, ponderomotive and thermal self-focusing.[21,22] This problem of self-focusing in the transition period during which the plasma profile begins to respond to ponderomotive forces and thermal heating will be addressed in a later paper.

The analysis presented here will be concerned only with relativistic self-focusing on a time scale sufficiently short so that the plasma density profile does not evolve significantly under the influence of the radiation beam. This implies that the pulse length of the radiation beam, τ_L, must be short compared to τ_S and, of course, long compared to a radiation period, τ_R.

The relativistic self-focusing effect is analyzed for a helically polarized beam propagating in the z direction. The beam is assumed to be axially symmetric with respect to the z axis and has a profile which is only a function of r,z and t. An equation which describes the envelope of the radiation beam is derived. The envelope equation includes diffraction effects as well as relativistic plasma effects and has a form similar to a particle beam envelope equation.[23,24] In the present radiation beam envelope equation, diffraction effects are manifested through a term which is equivalent to beam emittance in the particle beam envelope equation.

[illegible]

Consider a helically polarized radiation beam propagating within a cold collisionless plasma. The vector potential of the field is taken to have the form

$$A_L(r,z,t) = A(r,z)\left[\cos(kz-\omega t)\hat{e}_x - \sin(kz-\omega t)\hat{e}_y\right], \qquad (1)$$

where the amplitude $A(r,z)$ is a slowly varying function of r and z, and the frequency ω is assumed to be much greater than the effective plasma frequency. The approximate local dispersion relation associated with the field in (1) is

$$\omega = ck + \left(c^2k_\perp^2 + \omega_p^2(r,z)\right)/2ck, \qquad (2)$$

where $k_\perp = \left(k_x^2 + k_y^2\right)^{1/2}$ is the transverse wave number, $k_\perp^2 \ll k^2$ and $\omega_p^2(r,z)$ is the effective background plasma frequency. For purposes of this discussion the effective plasma frequency is written in the form

$$\omega_p^2(r,z) = \frac{n(r,z)}{n_o}\,\frac{\omega_{po}^2}{\gamma_\perp(r,z)}, \qquad (3)$$

where $\omega_{po} = (4\pi|e|^2 n_o/m_o)^{1/2}$ is the ambient plasma frequency, $n(r,z)$ is the modified electron density of the plasma due to the excited plasma wave, $\gamma_\perp(r,z) = \left(1+a^2(r,z)\right)^{1/2}$ is the relativistic mass factor and $a(r,z) = |e|A(r,z)/m_oc^2$ is the normalized laser field amplitude. The relativistic factor $\gamma_\perp$ arises from the plasma electrons' relativistic mass change due to their transverse oscillations in the radiation field.

Using the ray equations from geometric optics, the transverse motion of the electromagnetic rays are given by

$$\frac{d}{dt}\underset{\sim}{r}_{\perp} = \frac{\partial \omega}{\partial \underset{\sim}{k}_{\perp}} \tag{4a}$$

$$\frac{d}{dt}\underset{\sim}{k}_{\perp} = -\frac{\partial \omega}{\partial \underset{\sim}{r}_{\perp}}, \tag{4b}$$

where $\underset{\sim}{r}_{\perp} = \tilde{x}(t)\hat{e}_x + \tilde{y}(t)\hat{e}_y$ is the transverse position of a ray, $\underset{\sim}{k}_{\perp} = k_x(t)\hat{e}_x + k_y(t)\hat{e}_y$ is the transverse wave number of a ray and ω is given by (2). Substituting (2) into (4a) and (4b) yields the transverse ray equations

$$\frac{d^2\tilde{x}}{dt^2} + \Omega^2(\tilde{r},\tilde{z})\tilde{x} = 0, \tag{5a}$$

$$\frac{d^2\tilde{y}}{dt^2} + \Omega^2(\tilde{r},\tilde{z})\tilde{y} = 0, \tag{5b}$$

where

$$\Omega^2(r,z) = \frac{1}{2k^2 r}\frac{\partial \omega_p^2(r,z)}{\partial r}, \tag{5c}$$

and

$$\frac{\partial \omega_p^2}{\partial r} = \omega_{po}^2 \frac{\partial}{\partial r}\frac{n(r,z)/n_o}{(1+a^2(r,z))^{1/2}}. \tag{5d}$$

Equations (5a,b) describe the transverse motion of the rays and assume that the rays travel nearly parallel to the z axis, i.e., $|dx/dt|, |dy/dt| \ll v_g = c$ where v_g is the group velocity.

Derivation of Radiation Beam Envelope Equation

In this section an envelope equation is derived which describes the transverse dynamics of the radiation beam envelope as it propagates through a plasma. The derivation is similar to that used to obtain a particle beam envelope equation[24] in the sense that the ray equations in (5a,b) have a form which is similar to particle orbits in the paraxial approximation.

To this end, various moments are taken of the ray equations given by (5). Multiplying (5a) by $\tilde{x}$ and $d\tilde{x}/dt$, (5b) by $\tilde{y}$ and $d\tilde{y}/dt$ and combining, yields the following virial and energy equations

$$\frac{1}{2}\frac{d^2\tilde{r}^2}{dt^2} - \tilde{v}^2 + \Omega^2(\tilde{r},\tilde{z})\tilde{r}^2 = 0, \tag{6a}$$

$$\frac{d\tilde{v}^2}{dt^2} + \Omega^2(\tilde{r},\tilde{z})\frac{d\tilde{r}^2}{dt} = 0, \tag{6b}$$

where $\tilde{r}^2 = \tilde{x}^2 + \tilde{y}^2$ and $\tilde{v}^2 = (d\tilde{x}/dt)^2 + (d\tilde{y}/dt)^2$. Substituting (6a) into (6b) yields

$$\frac{1}{2}\frac{d^3\tilde{r}^2}{dt^3} + \frac{d}{dt}(\Omega^2\tilde{r}^2) + \Omega^2\frac{d\tilde{r}^2}{dt} = 0. \tag{7}$$

To obtain the envelope equation, consider a thin slice of the beam lying in the transverse. The transverse segment of the beam is assumed to consist of N individual rays traveling through it. The mean square radius of the radiation beam envelope is then defined as

$$R^2(\tilde{z},t) = \langle\tilde{r}^2\rangle = \frac{1}{N}\sum_{i=1}^{N}\tilde{r}_i^2 \tag{8}$$

where $\tilde{r}_i$ is the radial position of the ith ray and < > denotes the averaging operation. Mathematically, this averaging can be written in terms of an integral over the distribution function of initial ray positions at the initial time t_o, $f(\tilde{r}_o, t_o)$.

$$\langle Q(\tilde{r})\rangle = \int_o^\infty d\tilde{r}_o \tilde{r}_o f(\tilde{r}_o, t_o) Q(\tilde{r}), \tag{9}$$

where $Q(\tilde{r})$ is a quantity dependent on the ray position $\tilde{r} = \tilde{r}(\tilde{r}_o, t)$. Performing this average over all the rays on (7) and using (8) gives

$$\frac{1}{2}\frac{d^3R^2}{dt^3} + \frac{d}{dt}\langle \Omega^2 \tilde{r}^2\rangle + \langle \Omega^2 \frac{d\tilde{r}^2}{dt}\rangle = 0. \tag{10}$$

In order to express the averages in (10) in a more manageable form, the individual radial ray velocity is written as a sum of a mean velocity term and a residual velocity term. That is the individual ray velocity is written as

$$\tilde{v} = \frac{\tilde{r}}{R}\frac{dR}{dt} + \delta\tilde{v}, \tag{11}$$

where $(\tilde{r}/R)dR/dt$ is defined as the mean radial velocity at the ray position $\tilde{r}$ and $\delta\tilde{v}_r$ is the residual radial velocity. Substituting (11) into the last term in (10) yields

$$\langle \Omega^2 \frac{d\tilde{r}^2}{dt}\rangle = 2\langle \Omega^2 \tilde{r}^2\rangle \frac{dR/dt}{R} + 2\langle \Omega^2 \tilde{r}\delta\tilde{v}_r\rangle. \tag{12}$$

To further simplify (12), notice that

$$\frac{1}{2}\frac{d}{dt}R^2 = \frac{1}{2}\frac{d}{dt}\langle\tilde{r}^2\rangle$$

$$= \langle\tilde{v}\tilde{r}\rangle = R\frac{dR}{dt} + \langle\tilde{r}\delta\tilde{v}\rangle. \qquad (13)$$

Hence, $\langle\tilde{r}\delta\tilde{v}\rangle = 0$. Similarly, assuming $\langle\tilde{r}^n\rangle = c_n R^n$ where c_n is a constant, then

$$\frac{1}{n}\frac{d}{dt}R^n = \frac{1}{n}\frac{d}{dt}\langle\tilde{r}^n\rangle$$

$$= \langle\tilde{r}^{n-1}\,\tilde{v}\rangle = c_n R^{n-1}\frac{dR}{dt} + \langle\tilde{r}^{n-1}\delta\tilde{v}\rangle. \qquad (14)$$

Hence, the conclusion is reached that $\langle\tilde{r}^m\delta\tilde{v}\rangle = 0$ for any positive integer m.

Assuming that $\Omega^2(r)$ can be expanded in a power series of r implies that $\langle\Omega^2\tilde{r}\delta\tilde{v}\rangle = 0$. Thus, (12) becomes

$$\langle\Omega^2\frac{d\tilde{r}^2}{dt}\rangle = 2\langle\Omega^2\tilde{r}^2\rangle\frac{1}{R}\frac{dR}{dt}. \qquad (15)$$

Substituting (15) into (10) yields

$$\frac{1}{2}\frac{d^3R^2}{dt^3} + \frac{d}{dt}\langle\Omega^2\tilde{r}^2\rangle + 2\langle\Omega^2\tilde{r}^2\rangle\frac{dR/dt}{R} = 0. \qquad (16)$$

Since the last two terms in (16) combine to give $R^{-2}d(R^2\langle\Omega^2\tilde{r}^2\rangle)/dt$, (16) can be written as

$$\frac{d}{dt}\left[R^2\frac{d^2R^2}{dt^2} - \frac{1}{2}\left(\frac{dR^2}{dt}\right)^2 + 2R^2\langle\Omega^2\tilde{r}^2\rangle\right] = 0. \qquad (17)$$

Integrating (17) and taking the constant of integration to be $2c^2\epsilon^2$ gives

$$\frac{d^2R}{dz^2} + \frac{\langle K^2\tilde{r}^2\rangle}{R} - \frac{\epsilon^2}{R^3} = 0, \tag{18}$$

where $K^2 = \Omega^2/c^2$ and $z = ct$.

Equation (18) describes the evolution of the radiation beam envelope, R, as function of z. Diffraction effects which result in a spreading of the beam are contained in the constant of integration term ϵ. The form of the envelope equation for the radiation beam, (18), is similar to the usual particle beam envelope equation. The second term in (18) can be either focusing or defocusing depending on the sign of Ω^2. In the present situation, because of the relativistic transverse oscillations of the background plasma electrons, this term results in focusing of the radiation beam. The third term in (18) is always a defocusing term and is due to diffraction effects.

The diffraction constant ϵ^2 can be evaluated for the special case of a Gaussian ray distribution. Using the definition in (9) and requiring $\langle 1\rangle = 1$ and $\langle\tilde{r}^2\rangle = R^2$ then implies

$$f(\tilde{r}_o,t_o) = \frac{2}{R^2}\, e^{-\tilde{r}_o^{\,2}/R^2}. \tag{19}$$

Since the density of rays is proportional to the intensity of the radiation field, this implies that $f(\tilde{r}_o,t_o)$ is proportional to $a^2(\tilde{r}_o,t)$. In standard notation, the vector potential of a Gaussian radiation field is written as

$$a(r,z) = \frac{a_o R_{so}}{R_s(z)}\, e^{-r^2/R_s^2}, \tag{20}$$

where $R_s(z)$ is the spot size, R_{so} the minimum spot size and a_o is the normalized peak radiation amplitude. In a vacuum, $R_s(z)$ is given by

$$R_s(z) = R_{so}\left[1 + \frac{(z-z_o)^2}{z_R^2}\right]^{1/2}, \qquad (21)$$

where $z_R = kR_{so}^2/2$ is the Rayleigh length[25] and z_o is the axial location of the minimum spot size.

Since $f(\tilde{r}_o, t_o)$ is proportional to $a^2(\tilde{r}_o, t)$, then by comparing (19) and (20) implies that the mean-square radial ray position is related to the spot size by $R^2 = R_s^2/2$. Rewriting the envelope equation (18) in terms of the spot size R_s gives

$$\frac{d^2R_s}{dz^2} + \frac{2\langle\tilde{r}^2K^2\rangle}{R_s} - \frac{\varepsilon_o}{R_s^3} = 0. \qquad (22)$$

The integration constant ε_o can now be evaluated by using the vacuum solution (21). In vacuum, $\langle\tilde{r}^2K^2\rangle = 0$ and, hence, $\varepsilon_o^2 = 4/k^2$. Notice that $\varepsilon_o = \lambda/\pi = R_{so}\theta_d$, where $\lambda = 2\pi/k$ and $\theta_d = \lambda/(\pi R_{so})$ is the well-known diffraction angle.[25]

Solution of Envelope Equation

In order to solve the envelope equation (22) it is necessary first to evaluate the average of the quantity $\tilde{r}^2K^2$, where

$$\tilde{r}^2K^2 = \frac{\omega_{po}^2}{2c^2k^2}\,\tilde{r}\,\frac{\partial}{\partial\tilde{r}}\,\frac{n(\tilde{r},\tilde{z})/n_o}{\left(1 + a^2(\tilde{r},\tilde{z})\right)^{1/2}}, \qquad (23)$$

where $\tilde{r} = \tilde{r}(\tilde{r}_o, t)$ and $\tilde{z} = ct + \tilde{z}_o$.

Recall that the averaging can be written in terms of the distribution of initial ray positions $f(\tilde{r}_o, t_o)$ as in (9). Notice that it is possible to define a Eulerian ray distribution function at position r and time t as follows:

$$f(r,t) = \int_0^\infty d\tilde{r}_o f(\tilde{r}_o,t)\delta(r - \tilde{r}(\tilde{r}_o,t)). \tag{24}$$

Consider now the average of the quantity Q(r) defined by

$$\begin{aligned}
\langle Q(r)\rangle &= \int_0^\infty dr\, r f(r,t) Q(r) \\
&= \int_0^\infty dr\, r \int_0^\infty d\tilde{r}_o f(\tilde{r}_o,t)\delta(r - \tilde{r}(\tilde{r}_o,t)) Q(r) \\
&= \int_0^\infty d\tilde{r}_o \tilde{r}_o f(\tilde{r}_o,t) Q(\tilde{r}) \\
&= \langle Q(\tilde{r})\rangle.
\end{aligned} \tag{25}$$

Hence, the averaging $\langle Q(\tilde{r})\rangle$ can be replaced by an integration over the Eulerian spatial coordinate r providing the distribution f(r,t) is known.

Since there is no hope in determining an analytic expression for the distribution f(r,t), in order to obtain an estimate of $\langle \tilde{r}^2 K^2\rangle$, it will be assumed that the radiation beam retains a Gaussian profile as it propagates through the plasma. Thus, f(r,t) will be approximated as

$$f(r,z) = \frac{4}{a_o^2 R_{so}^2}\, a^2(r,z), \tag{26}$$

where $z = ct + z_o$ and a(r,z) is given by (20). Notice that $\langle 1\rangle = 1$ and $\langle r^2\rangle = R_s^2/2$. Using this expression, then $\langle r^2K^2\rangle$ becomes

$$\begin{aligned}
\langle r^2K^2\rangle &= 2\left(\frac{\omega_{po}}{cka_oR_{so}}\right)^2 \int_0^\infty dr\, r^2 a^2(r,z)\, \frac{\partial}{\partial r}\, \frac{n(r,z)/n_o}{(1+a^2(r,z))^{1/2}} \\
&= -\left(\frac{\omega_{po}}{ck}\right)^2 \int_0^\infty ds(1-s)e^{-s}\, \frac{n(s)/n_o}{(1+x^{-2}e^{-s})^{1/2}},
\end{aligned} \tag{27}$$

where $\xi = \gamma r^2/R_s^2$ and $x = R_s/(R_{so}a_o)$.

For the case of a constant density background plasma, $n(r) = n_o$ for $r < R_p$ and $n(r) = 0$ for $r > R_p$, then (27) can be evaluated analytically. For this case, letting $y = e^{-\xi}$, then

$$\langle r^2k^2\rangle = \frac{\omega_{po}^2}{c^2k^2}\int_1^{y_p}\frac{dy(1+\ell ny)}{(1+x^{-2}y)^{1/2}}$$

$$= \frac{4\omega_{po}^2}{c^2k^2}x^2\left[h(x) - g(x)(1-\ell ny_p) - \ell n\left[\frac{1+h}{1+g}\right]\right], \qquad (28)$$

where $h = [(1+x^{-2})^{1/2}-1]/2$, $g = [(1+x^{-2}y_p)^{1/2}-1]/2$ and $y_p = \exp(-2R_p^2/R_s^2)$.

It is insightful to write the envelope equation in terms of an effective particle located at $R_s(z)$ moving in a potential $V(R_s)$. Equation (22) becomes

$$\frac{d^2R_s}{dz^2} = -\frac{\partial V(R_s)}{\partial R_s}, \qquad (29)$$

where

$$\frac{\partial V}{\partial R_s} = \frac{8\omega_{po}^2}{c^2k^2}\frac{R_s}{a_o^2R_{so}^2}\left[h(x) - g(x)(1-\ell ny_b) - \ell n\left(\frac{1+h}{1+g}\right)\right] - \frac{4}{k^2R_s^3}, \qquad (30)$$

with $x = R_s/(a_oR_{so})$ and $y_p = \exp(-2R_p^2/R_s^2)$.

Envelope Behavior

To analyze the behavior of the radiation envelope, it is most convenient to use the normalized envelope radius $x = R_s/(a_oR_{so})$. In the limit $R_p \to \infty$, then (30) can be written as

$$\frac{d^2}{dt^2}x = -V_o\frac{\partial}{\partial x}V, \qquad (31)$$

where

$$-\frac{\partial}{\partial x} V = x^{-3} - 16\alpha x[((1 + x^{-2})^{1/2} - 1) + 2\ell n2$$

$$- 2\ell n((1+x^{-2})^{1/2} + 1)], \quad (32)$$

with

$$V_o = (2c/(kR_{so}^2 a_o^2))^2 \text{ and } \alpha = (\omega_{po} a_o R_{so}/(4c))^2.$$

The above equation describes the position of a particle x(t) moving in the effective potential V(x,α). In the expression for ∂V/∂x, the first term on the right of (32) represents vacuum diffraction whereas the term proportional to α represents the relativistic self-focusing of the plasma.

It is interesting to note that the shape of the potential V(x) depends only on the parameter α. As will be shown below, α can be written as the laser power over the critical power. For α > 1, the potential V(x) has a minimum and bounded oscillatory solutions for x(t) are possible.

Expanding V(x) for large x (small a_o) gives

$$\frac{\partial V}{\partial x} = x^{-3} - \alpha x^{-3}. \quad (33)$$

For α = 1, there are no net diffraction or focusing forces (to leading order) and a matched radiation beam is possible. In this limit (x >> 1), the envelope diffracts for α < 1 and focuses for α > 1. Since the total radiation power is given by $P = (m_e c^2 \omega a_o R_{so})^2/(8ce^2)$, the parameter α can be written as $\alpha = P/P_{crit}$, where the critical power is given by

$$P_{crit} = 2c\left(\frac{m_e c^2}{e}\right)^2 \frac{\omega^2}{\omega_{po}^2} = 17.4 \times 10^9 \frac{\omega^2}{\omega_{po}^2} \text{ Watts}. \quad (34)$$

[illegible], $\omega/\omega_{pe} = 28$ gives $P_{crit} = 6 \times 10^{12}$ W.

Equation (33) indicates that for $x \gg 1$, and $\alpha > 1$, then the radiation will focus until $x \sim 1$ and (33) is no longer valid. Expanding (32) for small $x \ll 1$ gives

$$-\frac{\partial V}{\partial x} = x^{-3} - 16\alpha. \tag{35}$$

Equation (35) states that for a fixed $\alpha > 1$, focusing will continue until the diffraction term dominates when $x^3 < 1/(16\alpha)$. Hence, at a sufficiently small x, the envelope will be reflected back out towards its original width. When this occurs the envelope radius x will either oscillate between its minimum value at reflection and its original value, or it will continue to diffract indefinitely, depending on the envelope's initial "velocity" (the initial slope in x(t)). For a given $\alpha > 1$ and an initial $x \gg 1$, if the initial slope dx/dt is sufficiently small, then x(t) will oscillate between its initial value and its value at reflection. If dx/dt is initially large, x(t) will initially decrease to its minimum value at reflection and then increase indefinitely.

The exact shape of V(x) for a given α must be determined numerically. In general, if $\alpha > 1$ then there will exist a finite well whose minimum occurs at x_f. As α increases, the depth of this well increases, the well becomes narrower and the location of the minimum x_f decreases. The potential V(x) is plotted in Fig. 1 for $\alpha = 5.0$ and Fig. 2 for $\alpha = 1.2$. Notice that $x_f = 0.4$ for $\alpha = 5.0$ and $x_f = 1.8$ for $\alpha = 1.2$.

Recall from the vacuum solution that the minimum of R_s/R_{so} in vacuum is unity. Hence, the minimum for x in vacuum is $x = 1/a_o$. Ideally, it is possible to have a nonoscillating envelope of constant radius if the radiation

enters the plasma at $t = t_o$ with $x(t_o) = x_f$ and $dx/dt = 0$. This corresponds to the radiation entering the plasma precisely at the bottom of the potential well with zero velocity. In vacuum, $dx/dt = 0$ at the minimum spot size $R_s = R_{so}$ and, hence, $x = 1/a_o$. In order to achieve a nonoscillating solution, it is required that $x(t_o) = x_f = 1/a_o$. Hence, for $\alpha = 5.0$ ($\alpha = 1.2$) a nonoscillating matched beam would be possible for $a_o = 2.5$ ($a_o = 0.55$) provided the radiation envelope enters the plasma with zero slope, $dR_s/dz = 0$. Since current technology limits $a_o \leq 1$, operation in this constant envelope mode is possible only for α slightly greater than unity.

In practice, it may not be possible to achieve a radiation beam which enters a plasma with $dR_s/dz = 0$ and $x = x_f$. However, it may be possible to operate near $x = x_f$ with a small initial dx/dt. In this case, when $x = x_f + \delta x$ with δx small, the envelope equation (31) can be expanded to give

$$\frac{d^2}{dt^2}\delta x = -\omega_{os}^2 \delta x, \tag{36}$$

where

$$\omega_{os}^2 = -\frac{4V_o}{x_f^4}\left[1 - 4\alpha x_f^3 \frac{\left(\sqrt{1+x_f^2} - x_f\right)}{\left(1+x_f^2 + x_f\sqrt{1+x_f^2}\right)}\right]. \tag{37}$$

For the parameters $\alpha = 1.2$, $a_o = 0.55$, $R_{so} = 0.1$ cm and $\omega/\omega_{po} = 10$, this gives $x_f = 1.8$, $\lambda_{os} = 2\pi c/\omega_{os} = 43.5$ cm and $\omega_{os}^2/\omega_{po}^2 = 3 \times 10^{-6}$. The Rayleigh length for this case is $Z_R = 4.0$ cm.

Figures 3-6 show numerical results for the envelope behavior for a test case where $\alpha = 1.2$, $R_{so} = 0.1$ cm and $\omega/\omega_{po} = 10.0$. The critical power is given by $P_{crit} = 17 \times 10^{11}$W, the well minimum occurs at $x_f = 1.8$ and the oscillating wavelength in the well is $\lambda_{os} = 44$ cm. Figure 3 shows operation at $a_o = 1/x_f = 0.55$ and with zero initial slope, $dR_s/dz = 0$. This is the condition for a nonoscillating matched beam. Here $P = 2.1 \times 10^{12}$W,

$\omega_{po} = 2.4 \times 10^{12} sec^{-1}$, $\omega = 2.4 \times 10^{13} sec^{-1}$ and the Rayleigh length is $z_R = 4.0$ cm. Figure 4 shows a case with a_o slightly less than $1/x_f = 0.55$ with zero initial slope, while Fig. 5 shows a case with $a_o = 0.55$ and a small initial slope. In both these cases, the envelope shows a small amplitude oscillation whose wavelength is given by $\lambda = \lambda_{os} = 44$ cm. Figure 6 presents a case where $a_o << 0.55$ (initially, $\hat{x} >> 1$) and with a significant initial slope. Here the initial slope is determined by specifying z_o where $R_s(z) = R_{so}(1 + z_o^2/z_R^2)^{1/2}$ before entering the plasma at $z = 0$. For this case, the radiation initially focuses down to a value significantly less than R_{so} ("over-focusing") and then is reflected and diffracts indefinitely.

When larger laser powers are used (larger values of α) the results are qualitatively similar except the potential well is now deeper, narrower and has a minimum occurring at a smaller value of x_f. For example, when $\alpha = 5$, $R_{so} = .1$ cm and $\omega/\omega_{po} = 10$, then $x_f = 0.41$ and $\lambda_{os} = 8.9$ cm. A nonoscillating matched beam requires $a_o = 2.5$ and no initial slope. For $\alpha_o = 2.5$, this gives $P_{crit} = 1.7 \times 10^{12}$W, $P = 8.7 \times 10^{12}$W, $\omega_{po} = 1.1 \times 10^{12} sec^{-1}$, $\omega = 1.1 \times 10^{13} sec^{-1}$ and $z_R = 1.8$ cm.

Numerical Simulation

In order to confirm the above results, the wave equation for the radiation is solved numerically. For a plasma with constant density, and a driving current that results from the relativistic electron oscillations, the wave equation can be written as

$$\left[\frac{1}{r}\frac{\partial}{\partial r} r \frac{\partial}{\partial r} + 2i \frac{\omega}{c}\frac{\partial}{\partial z}\right] a(r,z) = \frac{\omega_{po}^2}{c^2} \frac{a(r,z)}{(1+a^2)^{1/2}} , \qquad (38)$$

where the slowly varying amplitude approximation was used. This equation is solved numerically with 64 x 64 transverse Fourier modes.

The initial transverse radiation profile was a Gaussian with zero wavefront curvature. As the radiation propagated through the plasma, the profile developed finite but small amplitude "skirts" indicating higher order transverse Gaussian modes are involved. The 1/e radius (at which the amplitude is 1/e that on axis) is chosen to be the measure of the radiation envelope. This is plotted as a function of z in Fig. 7 for the case when the initial normalized envelope $x = R_s/(R_{so}a_o)$ is somewhat greater than that needed for a matched beam. Figure 7 indicates that the envelope oscillates about the predicted matched beam radius. The oscillatory behavior is no longer simply harmonic, as implied by the above theory, and the oscillation wavelength is approximately twice the predicted value. Notice that after the initial transient, the maximum of the envelope oscillation is only about 2/3 of the initial radius of the radiation. This discrepancy is probably due to the fact that the profile deviates from its initially Gaussian shape. For the case where the value of the initial normalized envelope x approaches that required for a matched beam, the oscillation amplitude becomes very small and the oscillatory behavior becomes more erratic.

In general, the numerical simulations support the conclusion that the radiation envelope oscillates about the value required for matched beam propagation.

Conclusion

The above results indicate that relativistic electron quiver motion leads to enhanced focusing of radiation beams. Physically, relativistic quivering of the electrons leads to an effective decrease in the plasma density via the electron plasma frequency, $\omega_{pe}^2 = n(r,z)\omega_{po}^2/(n_o\gamma_\perp)$ where $\gamma_\perp^2 = 1 + a^2(r,z)$. A radiation field $a^2(r,z)$ peaked on axis at $r = 0$ will produce an index of refraction profile $\eta(r,z)$ peaked on axis such that $\partial\eta/\partial r < 0$, where $\eta = ck/\omega = (1 - \omega_p^2(r,z)/\omega^2)^{1/2}$. Since $\partial\eta/\partial r < 0$, this implies focusing of the radiation beam.

The effects of relativistic self-focusing on the development of the radiation envelope $R_s(z)$ are best understood through the analogy of a single particle with orbit $R_s(z)$ moving in an effective potential $V(R_s)$. As discussed above, the shape of the potential V is determined by a single parameter $\alpha = P/P_{crit}$, where the critical power is given by $P_{crit} = 17 \times 10^9 (\omega/\omega_{po})^2$ Watts. Provided $\alpha > 1$ (laser power greater than the critical power), then there exists a minimum in the effective potential V located at $x_f = x_f(\alpha)$, where $x = R_s/(R_{so}a_o)$. As α is increased, the well depth increases and becomes narrower, and the location of the minimum x_f decreases. The existence of such a well implies that bounded solutions for $R_s(z)$ are possible where $R_s(z)$ oscillates between the two reflection points associated with the effective potential. For example, if $\alpha > 1$, a radiation beam entering the plasma with an initial value of x greater than x_f will initially begin to focus (x decreases). When this occurs, two outcomes are possible: i) the normalized envelope x(z) will continue to decrease to some minimum value at which it will be reflected and expand indefinitely, or ii) the envelope x(z) will remain bounded, oscillating indefinitely between the minimum reflection point and its initial value. The occurrence of one or the other of the above two cases depends on the initial "convergence angle" of the

envelope $x(z)$ as it enters the plasma or, more precisely, on the initial slope dR_s/dz. If dR_s/dz is too large then case i) occurs: the envelope is reflected and expands indefinitely. If the initial dR_s/dz is sufficiently small, then case ii) occurs: the envelope becomes trapped in the potential well and oscillates about the minimum x_f. Under a special set of initial conditions, $dR_s/dz = 0$ and $x = x_f$, it is possible to have a matched beam with a constant envelope.

The following approximations were made in this analysis: the mathematical model used in the above calculations was based on the ray equations of geometrical optics. These ray equations then used a dispersion relation for an electromagnetic wave in an unmagnetized plasma in which it was assumed $k^2 >> k_\perp^2$ and $\omega^2 >> \omega_p^2$. The radiation beam was initially assumed to be Gaussian and, furthermore, it was assumed to remain Gaussian as it propagated through the plasma, $a(r,z) = (a_o R_{so}/R_s)\exp(-r^2/R_s^2(z))$. The last approximation, which restricts the analysis to short pulses, assumes that the background plasma density remains constant and does not evolve under the influence of the transverse ponderomotive force. Such an approximation should be valid for short pulse times $\tau < R_o/C_s$.

The results discussed above are in qualitative disagreement with those of Schmidt and Horton,[20] who also analyzed relativistic self-focusing for short pulses. They found a similar expression for P_{crit}, beyond which self-focusing occurs. They claimed, however, that for $P > P_{crit}$ the radiation beam would collapse down to some minimum radius and neither oscillate nor reflect. This is similar to the results of Max et al.,[18] in which it was determined that self-focusing occurs when a certain threshold is surpassed. Their analysis, however, did not predict the envelope behavior once self-focusing occurs. The above numerical simulation of the wave equation indicates that the correct

envelope behavior is an oscillation about the value required for a matched beam.

The results of Felber,[16] which included relativistic focusing along with that of the equilibrium ponderomotive effect, are in qualitative agreement with those presented above. Specifically, Felber[16] found that the behavior of the radiation envelope could also be described as a particle in an effective potential. Provided the laser power was sufficiently high, the potential exhibited a minimum and, hence, either oscillating, bounded solutions or reflected, diverging solutions were possible. The critical power in Felber's case was similar to that found by Max,[15] $P_{crit} \approx 2 \times 10^4 T(ev)\omega^2/\omega_p^2$ Watts, which is typically less than that discussed above when the effects of ponderomotive focusing are neglected. The main limitation with the analysis of Felber[16] and Max[15] is that both used an equilibrium density response, $n \sim \exp(e\phi_p/T)$ where ϕ_p is the ponderomotive potential. Such an equilibrium density response is invalid for the leading segment of the radiation pulse.

Acknowledgments

The authors would like to thank A. C. Ting for providing the numerical simulation of the wave equation.

This work is sponsored by the U. S. Department of Energy, Office of Energy Research, under Interagency Agreement No. DE-AI05-83ER40117.

References

1. Laser Acceleration of Particles, AIP Conf. Proc. No. 91, Ed. by Paul J. Channell, American Institute of Physics, New York, 1982.

2. Challenge of Ultra-High Energies: Ultimate Limits, Possible Directions of Technology, an Approach to Collective Acceleration. ECFA Report 83/68 published by Rutherford Appleton Laboratory (1983).

3. T. Tajima and J. M. Dawson, Phys. Rev. Lett. 43, 267 (1979).

4. T. Tajima and J. M. Dawson, IEEE Trans. Nucl. Sci. NS-26, 4188 (1979).

5. C. Joshi, T. Tajima, J. M. Dawson, H. A. Baldis and N. A. Ebrahim, Phys. Rev. Lett. 47, 1285 (1981).

6. M. Ashour-Abdalla, J. N. Leboeuf, T. Tajima, J. M. Dawson and C. F. Kennel, Phys. Rev. A 23, 1906 (1981).

7. D. J. Sullivan and B. B. Godfrey, IEEE Trans. Nucl. Sci. NS-28, 3395 (1981).

8. J. D. Lawson, Rutherford Appleton Laboratory, Report RL-83-057, 1983.

9. R. Bingham, private communications (1983).

10. C. M. Tang, P. Sprangle and R. N. Sudan, Appl. Phys. Lett. 45, 375 (1984).

11. C. M. Tang, P. Sprangle and R. N. Sudan, Phys. Fluids 28, 1974 (1985).

12. C. Joshi, W. B. Mori, T. Katsouleas, J. M. Dawson, J. M. Kindel and D. W. Forslund, Nature 311, 525 (1984).

13. W. Horton and T. Tajima, Phys. Rev. A. 31, 3937 (1985).

14. T. Katsouleas and J. M. Dawson, Phys. Rev. Lett. 51, 392 (1983).

15. C. Max, Phys. Fluids 19, 74 (1976).

16. F. S. Felber, Phys. Fluids 23, 1410 (1980).

17. C. Joshi, C. E. Clayton and F. F. Chen, Phys. Rev. Lett. 48, 874 (1982).

18. C. Max, J. Arons and A. B. Langdon, Phys. Rev. Lett. 33, 209 (1974).

19. P. Sprangle and Cha-Mei Tang, Laser Acceleration of Particles, AIP Conf. Proc. No. 130, ed. by C. Joshi and T. Katsouleas, Amer. Inst. of Phys. New York, p. 156, 1985.

20. G. Schmidt and W. Horton, Comments of Plasma Physics, Vol. 9, p. 85 (1985).

21. D. A. Jones, E. L. Kane, P. Lalousis, P. Wiles and H. Hora, Phys. Fluids 25, 2295 (1982).

22. A. Schmitt and R. S. B. Ong, J. Appl. Phys. 54, 3003 (1983).

23. J. D. Lawson, The Physics of Charged-particle Beams, (Clarendon Press, Oxford, 1978) Chap. 4.

24. E. P. Lee and R. K. Cooper, Part. Accel. 7, 83 (1976).

25. A. Yariv, Intro. to Optical Electronics, (Holt, Rinehart and Winston, New York, 1976) 2nd Edition, Chap. 3.

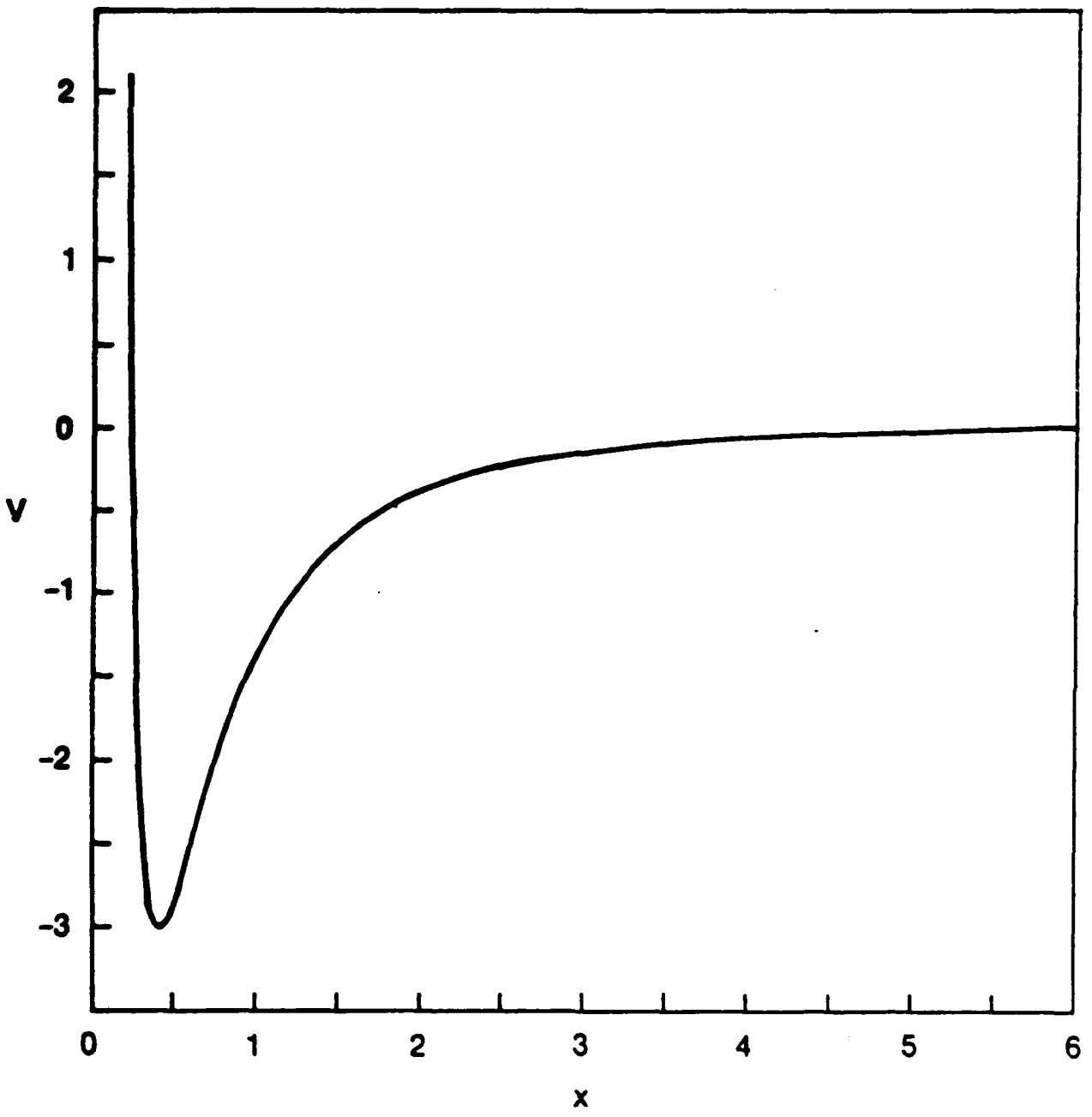

Figure 1. The effective potential V(x) as a function $x = R_s/(R_{so}a_o)$ for $\alpha = 5.0$. The well minimum occurs at $x_f = 0.4$.

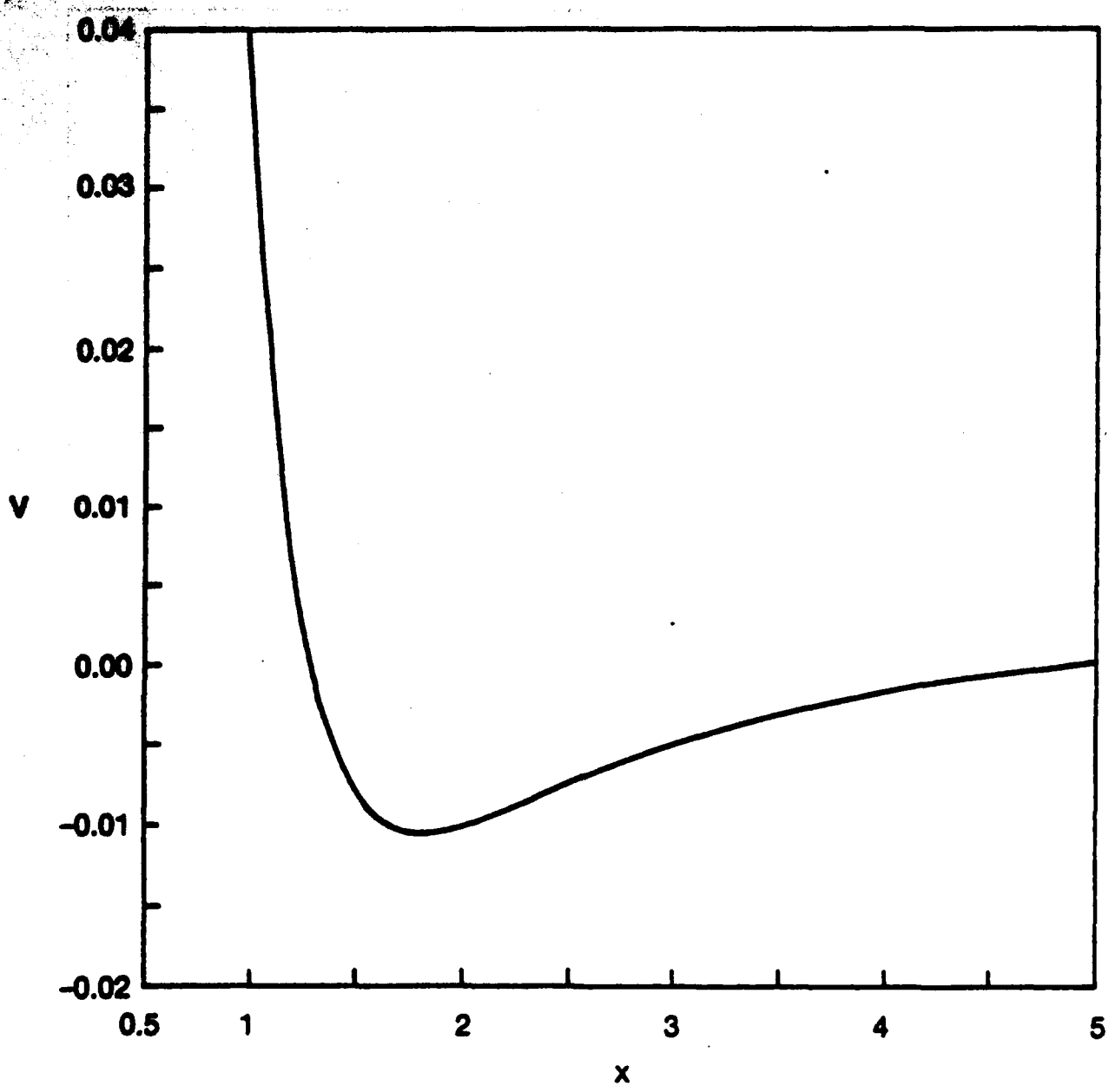

Figure 2. The effective potential V (x) as a function of $x = R_s/(R_{so}a_o)$ for $\alpha = 1.2$. The well minimum occurs at $x_f = 1.8$.

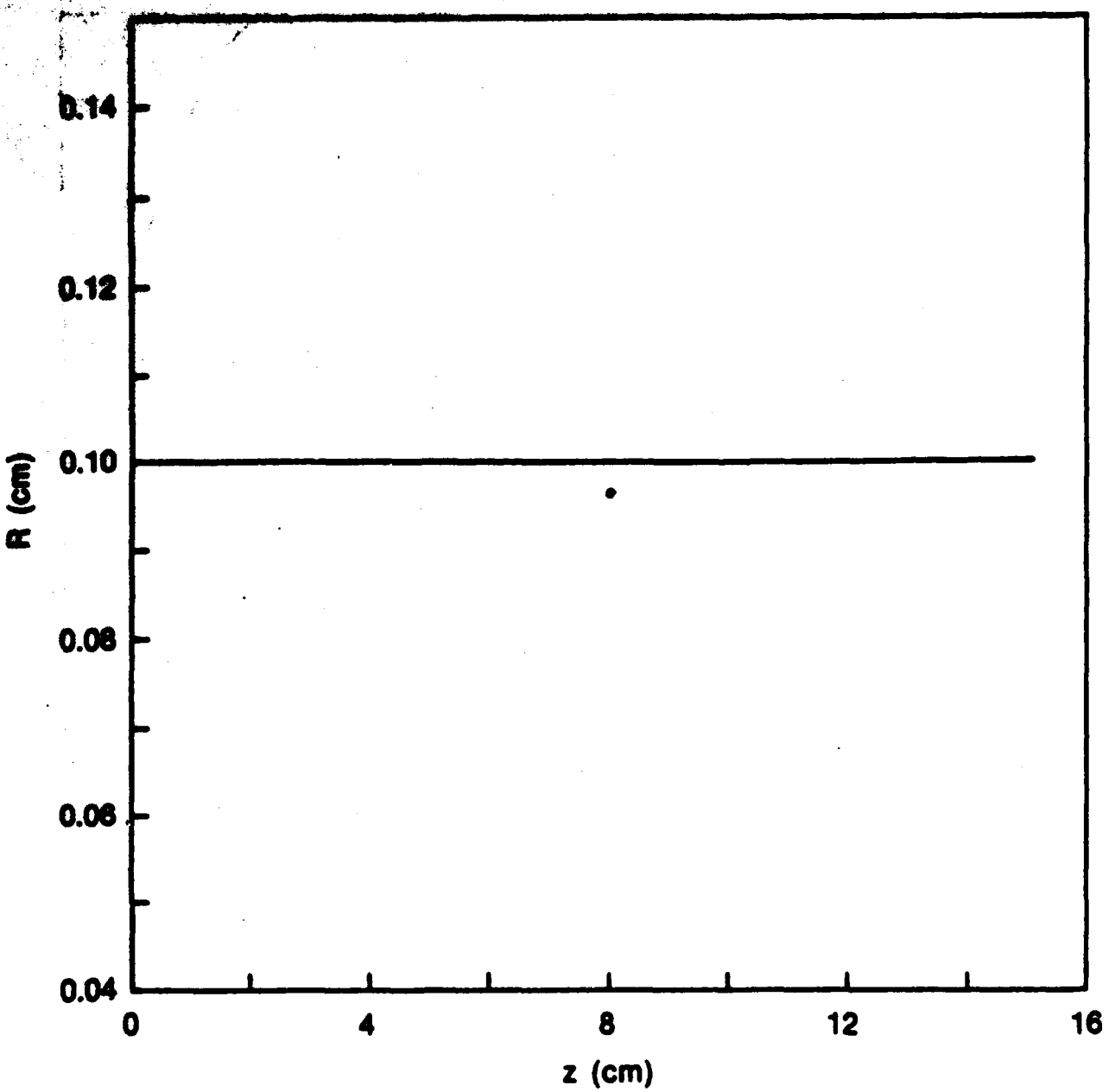

Figure 3. The radiation envelope $R_s(z)$ for the parameters $\alpha = 1.2$, $R_{so} = 0.1$ cm, $\omega/\omega_{po} = 10.0$ and $a_o = 0.55$. For this run $P_{crit} = 17 \times 10^{11}$ W and $\omega = 2.4 \times 10^{13} sec^{-1}$. Initially, $x = x_f = 1.8$ and $dx/dz = 0$.

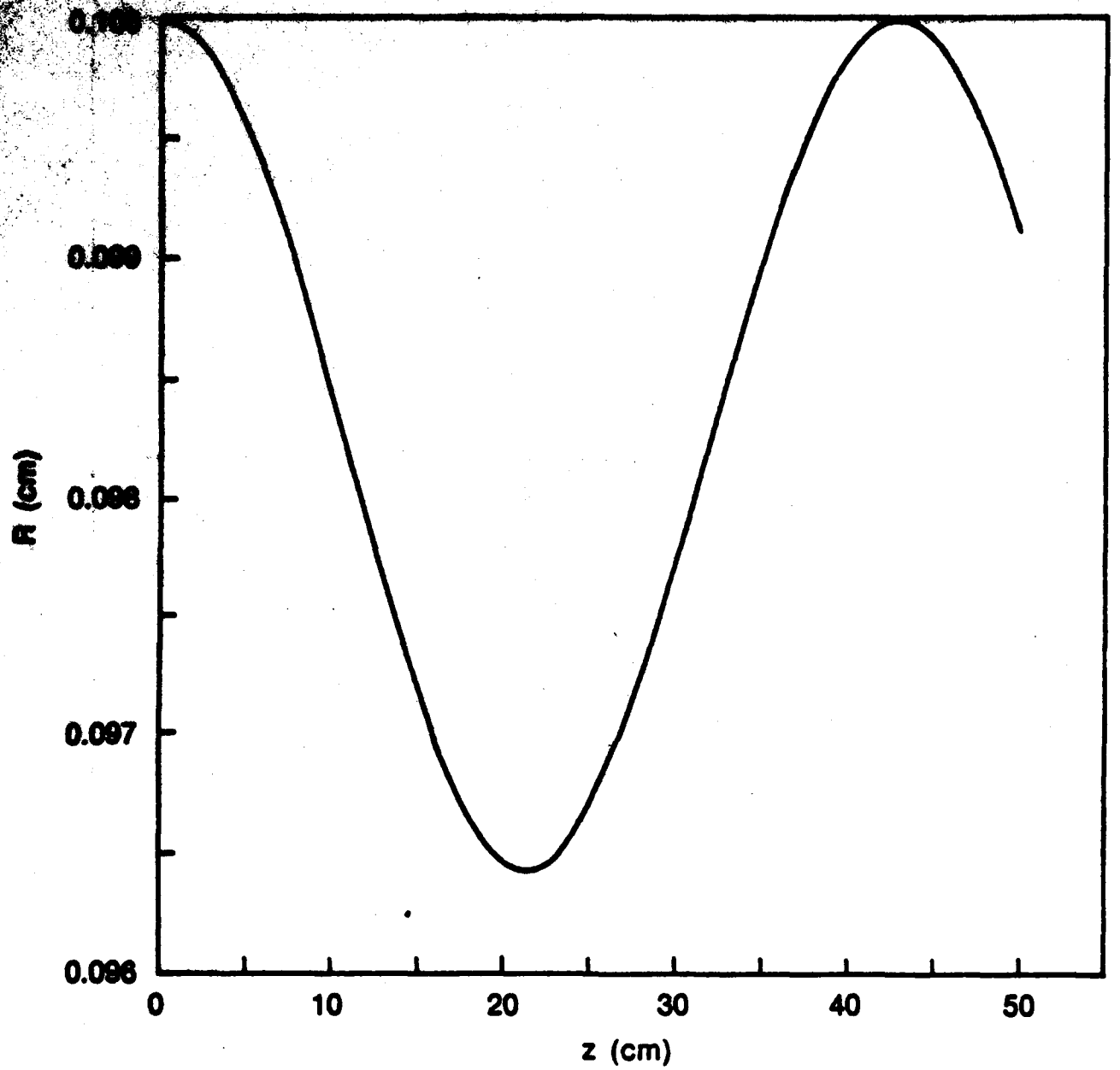

Figure 4. The radiation envelope $R_s(z)$ for the parameters a = 1.2, R_{so} = 0.1 cm, ω/ω_{po} = 10.0 and a_o = 0.54. For this run $P_{crit} = 17 \times 10^{11}$W, $\omega \sim 2.4 \times 10^{13} sec^{-1}$, z_R = 4.1 cm and λ_{os} = 44 cm. Initially, $x = 1.02\ x_f$ and dx/dz = 0.

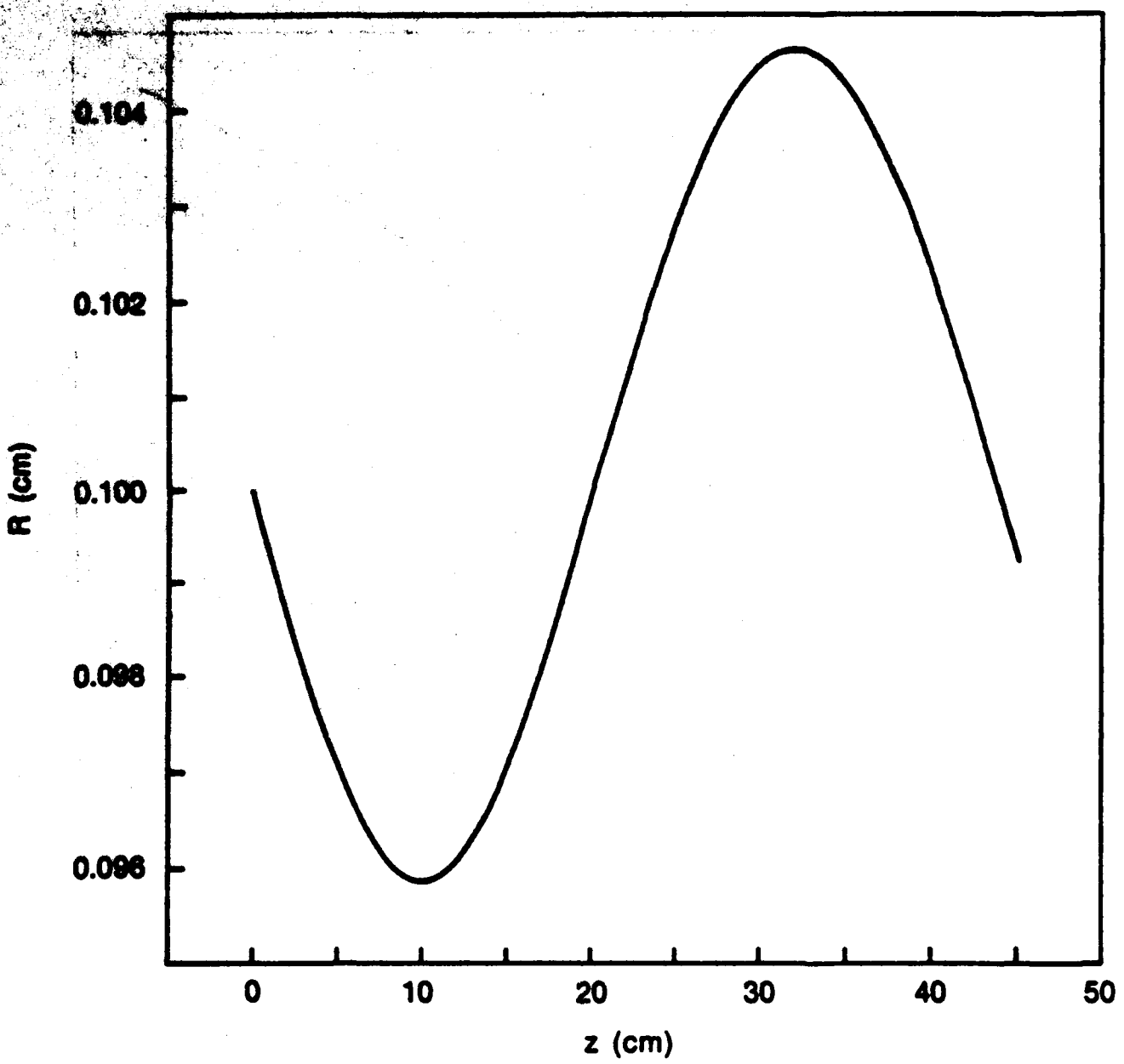

Figure 5. The radiation envelope $R_s(z)$ for the parameters, $\alpha = 1.2$, $R_{so} = 0.1$ cm, $\omega/\omega_{po} = 10.0$ and $a_o = 0.55$. For this run $P_{crit} = 17 \times 10^{11}$W, $\omega = 2.4 \times 10^{13} sec^{-1}$, $z_R = 4.0$ cm and $\lambda_{os} = 44$ cm. Initially, $x = x_f = 1.8$ with a small slope $dx/dz \neq 0$ ($dR_s/dz = R_{so} z_o / Z_R^2$, where $z_o = 0.1$ cm).

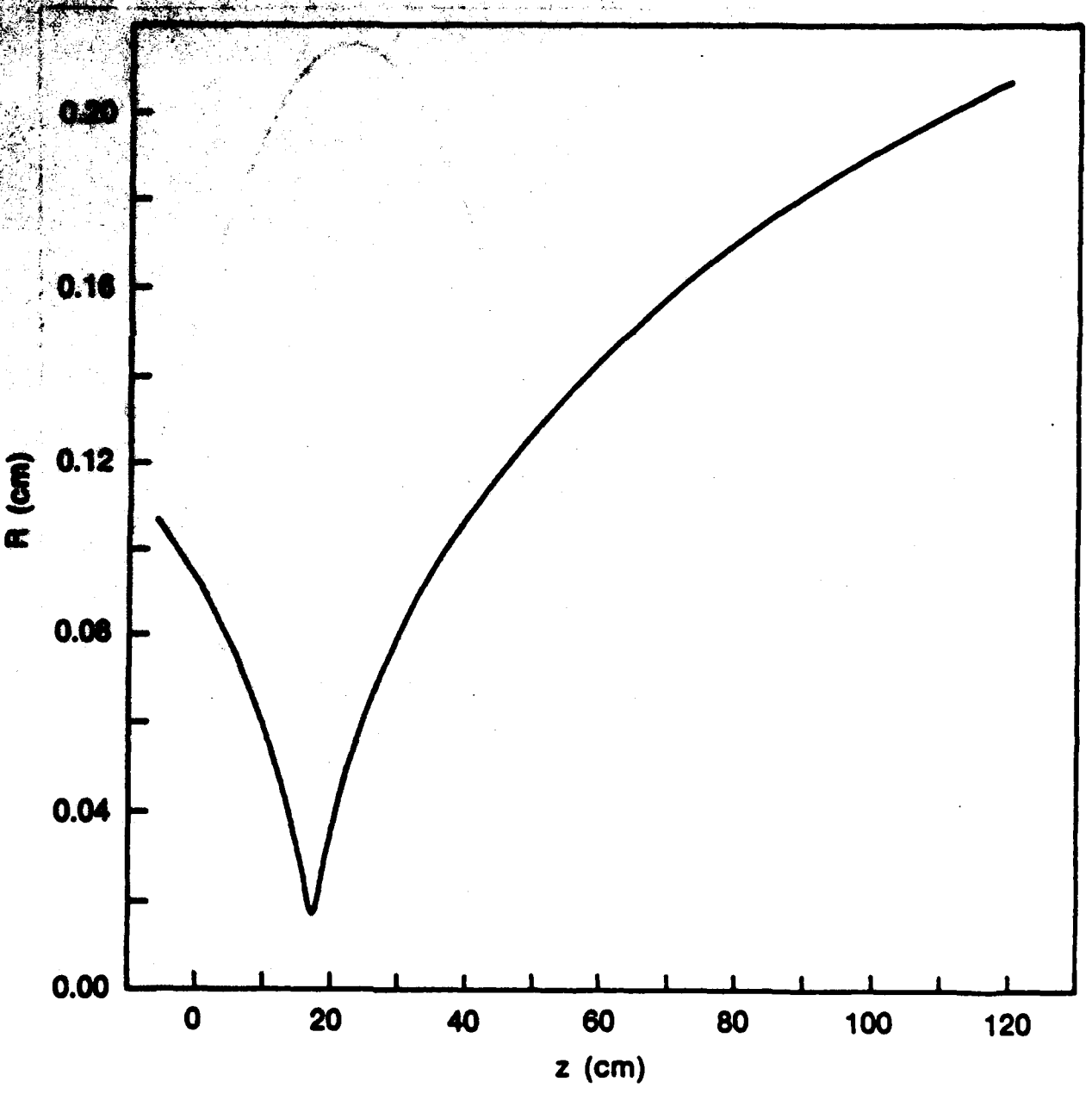

Figure 6. The radiation envelope $R_s(z)$ for the parameters $\alpha = 1.2$, $R_{so} = 0.1$ cm, $\omega/\omega_{po} = 10.0$ and $a_o = 0.14$. For this run $P_{crit} = 17 \times 10^{11}$W, $\omega = 9.4 \times 10^{13} sec^{-1}$ and $z_R = 16.0$ cm. Initially, $R_s = R_{so}(1 + z_o^2/z_R^2)^{1/2}$ with $z_o/z_R = 1/3$.

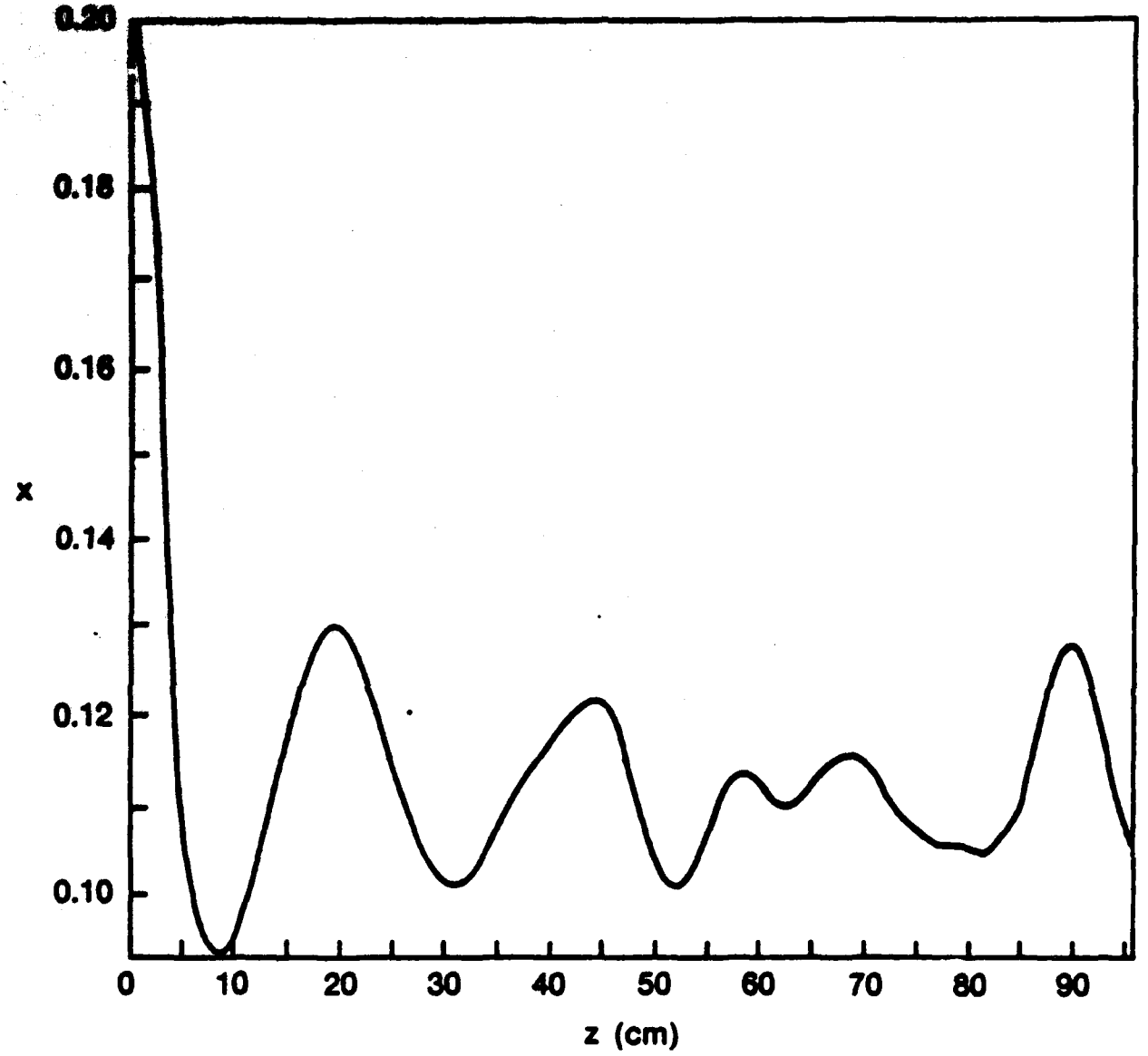

Figure 7. The 1/e radial width in terms of $x = R_s/(R_{so}a_o)$ as a function of z (in cm) as determined by numerical simulation of Eq. (38). For this run, $\alpha = 5$, $\omega/\omega_{po} = 10$, $a_o = 2.21$ and $R_{so} = 0.11$ cm.

DISTRIBUTION LIST

Naval Research Laboratory
4555 Overlook Avenue, S.W.
Washington, DC 20375-5000

Attn: Code 1000 - CAPT William C. Miller
1001 - Dr. T. Coffey
4603 - Dr. W.W. Zachary
4700 - Dr. S. Ossakow (26 copies)
4710 - Dr. J.A. Pasour
4710 - Dr. C.A. Kapetanakos
4740 - Dr. W.M. Manheimer
4740 - Dr. S. Gold
4790 - Dr. P. Sprangle (50 copies)
4790 - Dr. C.M. Tang (50 copies)
4790 - Dr. M. Lampe
4790 - Dr. Y.Y. Lau
4790A- W. Brizzi
4730 - Dr. R. Elton
6652 - Dr. N. Seeman
6840 - Dr. S.Y. Ahn
6840 - Dr. A. Ganguly
6840 - Dr. R.K. Parker (5 copies)
6850 - Dr. L.R. Whicker
6875 - Dr. R. Wagner
2628 - Documents (20 copies)
2634 - D. Wilbanks
1220 - 1 copy

Dr. R. E. Aamodt
Science Applications Intl. Corp.
1215 Walnut Street
Boulder, CO 80302

Dr. B. Amini
1763 B. H.
U. C. L. A.
Los Angeles, CA 90024

Dr. D. Bach
Los Alamos National Laboratory
P. O. Box 1663
Los Alamos, NM 87545

Dr. L. R. Barnett
3053 Merrill Eng. Bldg.
University of Utah
Salt Lake City, UT 84112

Dr. Peter Baum
General Research Corp.
P. O. Box 6770
Santa Barbara, CA 93160

Dr. Russ Berger
FL-10
University of Washington
Seattle, WA 98185

Dr. B. Bezzerides
MS-E531
Los Alamos National Laboratory
P. O. Box 1663
Los Alamos, NM 87545

Dr. Mario Bosco
University of California, Santa Barbara
Santa Barbara, CA 93106

Dr. Howard E. Brandt
Department of the Army
Harry Diamond Laboratory
2800 Powder Mill Road
Adelphi, MD 20783

Dr. Bob Brooks
FL-10
University of Washington
Seattle, WA 98195

Dr. Paul J. Channell
AT-6, MS-H818
Los Alamos National Laboratory
P. O. Box 1663
Los Alamos, NM 87545

Dr. A. W. Chao
Stanford Linear Accelerator Center
Stanford University
Stanford, CA 94305

Dr. Francis F. Chen
UCLA, 7731 Boelter Hall
Electrical Engineering Dept.
Los Angeles, CA 90024

Dr. K. Wendell Chen
Center for Accel. Tech.
University of Texas
P.O. Box 19363
Arlington, TX 76019

Dr. Pisin Chen
S.L.A.C.
Stanford University
P.O. Box 4349
Stanford, CA 94305

Major Bart Clare
USASDC
P. O. Box 15280
Arlington, VA 22215-0500

Dr. Christopher Clayton
UCLA, 7731 Boelter Hall
Electrical Engineering Dept.
Los Angeles, CA 90024

Dr. Bruce I. Cohen
Lawrence Livermore National Laboratory
P. O. Box 808
Livermore, CA 94550

Dr. B. Cohn
L-630
Lawrence Livermore National Laboratory
P. O. Box 808
Livermore, CA 94550

Dr. Richard Cooper
Los Alamos National Laboratory
P. O. Box 1663
Los Alamos, NM 87545

Dr. Paul L. Csonka
Institute of Theoretical Sciences
and Department of Physics
University of Oregon
Eugene, Oregon 97403

Dr. J. M. Dawson
Department of Physics
University of California, Los Angeles
Los Angeles, CA 90024

Dr. A. Dimos
NW16-225
M. I. T.
Cambridge, MA 02139

Dr. J. E. Drummond
Western Research Corporation
8616 Commerce Ave
San Diego, CA 92121

Dr. Frank Felber
Jaycor
11011 Torreyana Rd.
San Diego, CA 92121

Dr. H. Figueroa
308 Westwood Plaza, No. 407
U. C. L. A.
Los Angeles, CA 90024

Dr. Jorge Fontana
Electrical and Computer Engineering Dept.
University of California at Santa Barbara
Santa Barbara, CA 93106

Dr. David Forslund
Los Alamos National Laboratory
P. O. Box 1663
Los Alamos, NM 87545

Dr. John S. Fraser
Los Alamos National Laboratory
P.O. Box 1663, MS H825
Los Alamos, NM 87545

Dr. Dennis Gill
Los Alamos National Laboratory
P. O. Box 1663
Los Alamos, NM 87545

Dr. B. B. Godfrey
Mission Research Corporation
1720 Randolph Road, SE
Albuquerque, NM 87106

Dr. P. Goldston
Los Alamos National Laboratory
P. O. Box 1663
Los Alamos, NM 87545

Prof. Louis Hand
Cornell University
Ithaca, NY 14853

Dr. J. Hays
TRW
One Space Park
Redondo Beach, CA 90278

Dr. Wendell Horton
University of Texas
Physics Dept., RLM 11.320
Austin, TX 78712

Dr. J. Y. Hsu
General Atomic
San Diego, CA 92138

Dr. H. Huey
Varian Associates
B-118
611 Hansen Way
Palo Alto, CA 95014

Dr. Robert A. Jameson
Los Alamos National Laboratory
AT-Division, MS H811
P.O. Box 1663
Los Alamos, NM 87545

Dr. G. L. Johnston
NW16-232
M. I. T.
Cambridge, MA 02139

Dr. Shayne Johnston
Physics Department
Jackson State University
Jackson, MS 39217

Dr. C. Joshi
Electrical Engineering Department
University of California, Los Angeles
Los Angeles, CA 90024

Dr. E. L. Kane
Seience Applications Intl. Corp.
McLean, VA 22102

Dr. Tom Katsouleas
UCLA, 1-130 Knudsen Hall
Department of Physics
Los Angeles, CA 90024

Dr. Kwang-Je Kim
Lawrence Berkeley Laboratory
University of California, Berkeley
Berkeley, CA 94720

Dr. S. H. Kim
Center for Accelerator Technology
University of Texas
P.O. Box 19363
Arlington, TX 76019

Dr. Joe Kindel
Los Alamos National Laboratory
P. O. Box 1663, MS E531
Los Alamos, NM 87545

Dr. Ed Knapp
Los Alamos National Laboratory
P. O. Box 1663
Los Alamos, NM 87545

Dr. Norman M. Kroll
B-019
University of California, San Diego
La Jolla, CA 92093

Dr. Kenneth Lee
Los Alamos National Laboratory
P.O. Box 1663, MS E531
~~Los Alamos,~~ NM 87545

Dr. N. C. Luhmann, Jr.
7702 Boelter Hall
U. C. L. A.
Los Angeles, CA 90024

Dr. K. Maffee
University of Maryland
E. R. B.
College Park, MD 20742

Dr. B. D. McDaniel
Cornell University
Ithaca, NY 14853

Dr. Warren Mori
1-130 Knudsen Hall
U. C. L. A.
Los Angeles, CA 90024

Dr. P. L. Morton
Stanford Linear Accelerator Center
P. O. Box 4349
Stanford, CA 94305

Dr. Robert J. Noble
S.L.A.C., Bin 26
Stanford University
P.O. Box 4349
Stanford, CA 94305

Dr. Craig L. Olson
Sandia National Laboratories
Plasma Theory Division 1241
P.O. Box 5800
Albuquerque, NM 87185

Dr. H. Oona
MS-E554
Los Alamos National Laboratory
P. O. Box 1663
Los Alamos, NM 87545

Dr. Robert B. Palmer
Brookhaven National Laboratory
Upton, NY 11973

Dr. Richard Pantell
Stanford University
308 McCullough Bldg.
Stanford, CA 94305

Dr. Claudio Pellegrini
National Synchrotron Light Source
Brookhaven National Laboratory
Upton, NY 11973

Dr. Melvin A. Piestrup
Adelphi Technology
13800 Skyline Blvd. No. 2
Woodside, CA 94062

Dr. Z. Pietrzyk
FL-10
University of Washington
Seattle, WA 98185

Dr. Don Prosnitz
Lawrence Livermore National Laboratory
P. O. Box 808
Livermore, CA 94550

Dr. R. Ratowsky
Physics Department
University of California at Berkeley
Berkeley, CA 94720

Dr. Stephen Rockwood
Los Alamos National Laboratory
P. O. Box 1663
Los Alamos, NM 87545

Dr. R. D. Ruth
Lawrence Berkeley Laboratory
University of California, Berkeley
Berkeley, CA 94720

Dr. Al Saxman
Los Alamos National Laboratory
P.O. Box 1663, MS E523
Los Alamos, NM 87545

Dr. George Schmidt
Stevens Institute of Technology
Department of Physics
Hoboken, NJ 07030

Dr. N. C. Schoen
TRW
One Space Park
Redondo Beach, CA 90278

Dr. Frank Selph
U. S. Department of Energy
Division of High Energy Physics, ER-224
Washington, DC 20545

Dr. Andrew M. Sessler
Lawrence Berkeley Laboratory
University of California, Berkeley
Berkeley, CA 94720

Dr. Richard L. Sheffield
Los Alamos National Laboratory
P.O. Box 1663, MS H825
Los Alamos, NM 87545

Dr. John Siambis
Lockheed Missiles & Space Co.
Bldg. 205, Dept. 92-20
3251 Hanover Street
Palo Alto, CA 94304

Dr. Sidney Singer
MS-E530
Los Alamos National Laboratory
P. O. Box 1663
Los Alamos, NM 87545

Dr. E. Siusher
AT&T Bell Laboratories
Murray Hill, NJ 07974

Dr. Jack Slater
Spectra Technology
2755 Northup Way
Bellevue, WA 98009

Dr. Todd Smith
Hansen Laboratory
Stanford University
Stanford, CA 94305

Dr. Richard Spitzer
Stanford Linear Accelerator Center
P. O. Box 4347
Stanford, CA 94305

Prof. Ravi Sudan
Electrical Engineering Department
Cornell University
Ithaca, NY 14853

Dr. Don J. Sullivan
Mission Research Corporation
1720 Randolph Road, SE
Albuquerque, NM 87106

Dr. David F. Sutter
U. S. Department of Energy
Division of High Energy Physics, ER-224
Washington, DC 20545

Dr. T. Tajima
Department of Physics
and Institute for Fusion Studies
University of Texas
Austin, TX 78712

Dr. Lee Teng, Chairman
Fermilab
P.O. Box 500
Batavis, IL 60510

Dr. H. S. Uhm
Naval Surface Weapons Center
White Oak Laboratory
Silver Spring, MD 20903-5000

U. S. Naval Academy (2 copies)
Director of Research
Annapolis, MD 21402

Dr. John E. Walsh
Wilder Laboratory
Department of Physics (HB 6127)
Dartmouth College
Hanover, NH 03755

Dr. Tom Wangler
Los Alamos National Laboratory
P. O. Box 1663
Los Alamos, NM 87545

Dr. Perry B. Wilson
Stanford Linear Accelerator Center
Stanford University
P.O. Box 4349
Stanford, CA 94305

Dr. W. Woo
Applied Science Department
University of California at Davis
Davis, CA 95616

Dr. Wendell Worton
Institute for Fusion Studies
University of Texas
Austin, TX 78712

Dr. Jonathan Wurtele
M.I.T.
NW 16-234
Plasma Fusion Center
Cambridge, MA 02139

Dr. M. Yates
Los Alamos National Laboratory
P. O. Box 1663
Los Alamos, NM 87545

Dr. Ken Yoshioka
Laboratory for Plasma and Fusion
University of Maryland
College Park, MD 20742

Dr. R. W. Ziolkowski, L-156
Lawrence Livermore National Laboratory
P. O. Box 808
Livermore, CA 94550

DIRECTOR OF RESEARCH
U. S. NAVAL ACADEMY
ANNAPOLIS, MD 21402
2 COPIES

END

7-87

DTIC